GPS Error Correction With Pseudorange Evaluation Using Three-Dimensional Maps

Shunsuke Miura, Li-Ta Hsu, Feiyu Chen, and Shunsuke Kamijo, *Member, IEEE*

Abstract—The accuracy of the positions of a pedestrian is very important and useful information for the statistics, advertisement, and safety of different applications. Although the GPS chip in a smartphone is currently the most convenient device to obtain the positions, it still suffers from the effect of multipath and nonline-of-sight propagation in urban canyons. These reflections could greatly degrade the performance of a GPS receiver. This paper describes an approach to estimate a pedestrian position by the aid of a 3-D map and a ray-tracing method. The proposed approach first distributes the numbers of position candidates around a reference position. The weighting of the position candidates is evaluated based on the similarity between the simulated pseudorange and the observed pseudorange. Simulated pseudoranges are calculated using a ray-tracing simulation and a 3-D map. Finally, the proposed method was verified through field experiments in an urban canyon in Tokyo. According to the results, the proposed approach successfully estimates the reflection and direct paths so that the estimate appears very close to the ground truth, whereas the result of a commercial GPS receiver is far from the ground truth. The results show that the proposed method has a smaller error distance than the conventional method.

Index Terms—3-dimensional digital map, GNSS, GPS, non-line-of-sight (NLOS) propagation, ray tracing.

I. INTRODUCTION

PEDESTRIAN LOCALIZATION plays a very important role from the point of view of automated data collection for marketing surveys, statistics, and safety applications of intelligent transportation system (ITS). Global positioning system (GPS) is developed as a positioning technology and is widely used in various daily-use devices such as vehicles and cell phones. However, the positioning accuracy of a single frequency GPS receiver is currently not enough for the safety application of pedestrian such as pedestrian to vehicle (P2V) collision avoidance system and comfortable pedestrian positioning. The GPS receiver embedded in cell phones is usually low-cost, single-frequency, stand-alone modules. Its typical error budget is around 10 m drms [1], [2]. Although such performance is adequate for rough navigation, it is not sufficiently accurate from a safety perspective. Moreover, its positioning

performance is severely degraded in urban canyons. The main reason is the multipath effect and non-line-of-sight (NLOS) propagation. These effects may lead to a positioning error of around 100 m in urban canyons [3]. Various technologies are developed to mitigate the multipath and NLOS effects. Among these, special hardware-based correlator designed is proposed [4]–[9]. The idea of the hardware-based correlator design is to narrow the correlator spacing between channels. Thus, GPS receiver became more robust against multipath effect. The authors of this paper believe that the effect of the multipath is relatively small in comparison to NLOS reception. Therefore, this paper focuses on the detection of NLOS signals, and further increases the receiver positioning by taking advantage of NLOS reception.

Receiver autonomous integrity monitoring (RAIM) is a technology that could mitigate the multipath and NLOS problems [10], [11]. RAIM checks the residual of the least square during the positioning calculation and identifies suspicious satellites. RAIM then selects satellites in the calculation to minimize the least-square residual. Although RAIM is effective for the case of a few outliers, it is not fully appropriate for urban environments [12].

In recent years, various techniques have been developed to avoid NLOS satellites by an additional device or database for discrimination, such as using ray-tracing, omnidirectional cameras, referring the signal strength, dual-polarization antenna, or array antenna [12]–[19]. Peyret *et al.* [13] used digital maps to detect hidden satellites. Iwase *et al.* [12] used an altitude map to estimate the pseudorange error. Jiang *et al.* [19] used a dual-polarization antenna to accurately detect reflected signals, both in the form of NLOS reception and multipath interference, considering characteristics of circular polarization. Because the direct signals from GPS satellite are right-hand circular polarized (RHCP) whereas the reflected signals are left-hand circular polarized (LHCP), the dual-polarization antenna can separately compute the strength of RHCP signals and LHCP signals. Obst *et al.* [16] used a simple 3-D (3-D) ray-tracing method to distinguish NLOS satellites with small increase of calculation quantity. The 3-D environment model used in the 3-D ray-tracing method is created by integrating 2-D (2-D) building shapes, the terrain model, and the elevation model. The studies mentioned above reveal that the height data and additional devices to distinguish NLOS satellites is practical and very effective technique.

One of the most famous urban positioning method called, shadow matching, which uses city building models to predict the satellite visibility and compare it with measured satellite visibility to improve the cross street positioning accuracy

[20]–[22]. Recently, a real-time kinematic GNSS shadow matching based on particle filter is developed [23]. This kinematic GNSS shadow matching decides the likelihood of particles based on the signal strength and satellite visibility. The proposed method in this paper also applies particle filter to estimate receiver position. Moreover, this paper takes the advantage of 3-D map to generate the pseudorange correction for the purpose of correcting NLOS effect. As a result, the likelihood of the particle in this paper is determined by the similarity between corrected pseudorange and pseudorange measurement.

This study aims to improve the positioning accuracy of an inexpensive GPS module by discriminating NLOS satellites and calculating signal delays. By combining the ray-tracing simulation and 3-D building map, NLOS satellites are distinguished from all satellites perceived by a receiver with a small computational complexity. In addition, multipath effect is also mitigated by the examination of the receiver measurements. By the use of the NLOS satellite detection and multipath mitigation, this paper proposes an algorithm to accurately estimate positions on urban streets. The proposed method first distributes a number of positioning candidates and then evaluates the candidates' feasibility. The feasibility is determined by the 3-D map and ray-tracing technique. Afterwards, the calculation of proper likelihood function of the feasible candidates is achieved by the similarity of the simulated and receiver observed pseudorange. Finally, the expected value of all the candidates is regarded as the rectified receiver position.

II. GPS Receiver in Urban Canyon

A. Errors in GPS Measurement

This study uses a weighted least-squares (WLS) method for the positioning calculation, which is the standard algorithm for GPS positioning [1]. This method calculates the receiver position in three dimensions and the receiver clock offset according to the satellite positions obtained from the broadcast ephemeris. Thus, at least four pseudorange measurements from satellites are required to determine the receiver position and receiver clock offset. The measured raw pseudorange data are simply derived by multiplying the signal propagation time with the speed of light. Because the signal propagation time includes numerous delays, the associated corrections of the pseudorange must be calculated. Each pseudorange ρ_n is written as [1]

$$\rho_n = R_n + c\left(\delta t^{\mathrm{r}} - \delta t_n^{\mathrm{sv}}\right) + I_n + T_n + \varepsilon_n \tag{1}$$

where $R_n = \|\boldsymbol{x}_n^{\mathrm{sv}} - \boldsymbol{x}\|$ is the geometric range between the nth available satellite and the receiver, δt_n^{sv} denotes the satellite clock offset time; δt^{r}, the receiver clock offset time; I_n, the ionospheric delay distance; T_n, the tropospheric delay distance; and ε_n, the errors caused by the multipath, receiver noise, antenna delay, and so on. $\boldsymbol{\rho} = [\rho_1, \rho_2, \cdots, \rho_n]^T$ is the vector stacking all the available pseudorange measurements at one epoch. The error in measured pseudorange is caused by the delays mentioned above. Among them, ε is especially considered as a major cause of error because the other delays can be corrected by using appropriate models [1]. Therefore, the remaining error is mainly distributed by the multipath error and
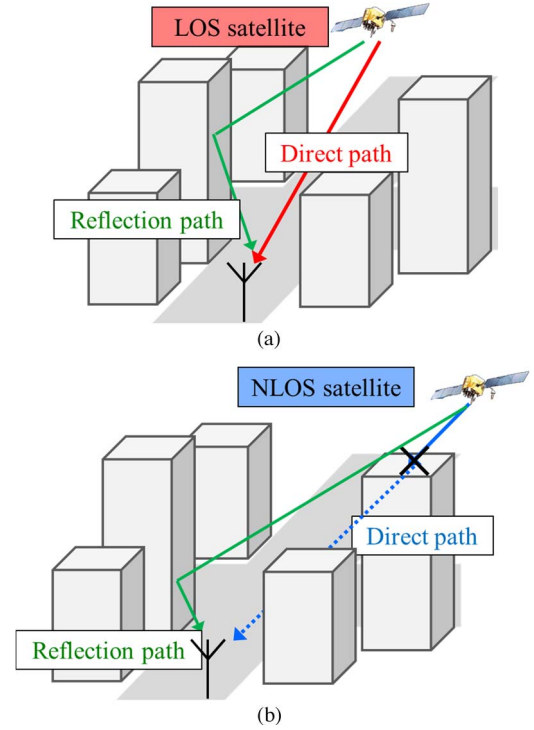

Fig. 1. The multipath and NLOS effects in an urban canyon. (a) Multipath effect. (b) NLOS propagation.

the receiver noise. Here, considering the noise is negligibly small, the dominant error is regarded as the multipath and NLOS error.

B. Introduction to Multipath and NLOS

Multipath effect denotes that there are two or more traveling paths of signal from one satellite to receivers. The direct signal is called the line of sight (LOS) signal, while the others are reflected signals. The reflection of signal often occurs in an environment with a lot of high buildings such as downtown. The urban environments contain many flat surfaces that may easily reflect the GPS signals. Fig. 1 illustrates an example of the reflecting effects in the environment of an urban canyon. As shown in Fig. 1, a multipath consists of a direct path (LOS) and reflected path, which makes the observed pseudorange longer than the real path. The worst case is NLOS reception, that is, only the reflected signal is received, while the direct path is blocked by some objects. These effects may lead to a positioning error of around 100 m in urban canyons [3]. The positioning errors caused by multipath and NLOS are very different in a conventional GPS receiver. The conventional GPS receiver utilizes a multipath mitigation based on the code-discriminator design.

As indicated in [15], the multipath effect can be corrected by the narrow correlator, which is a typical multipath mitigation correlator. The theoretical multipath envelop of the narrow correlator is shown in Fig. 2.

As shown in Fig. 2, the multipath delay in pseudorange domain is around 5 meter. However, the delay caused by NLOS cannot be mitigated by such discriminator-based method.
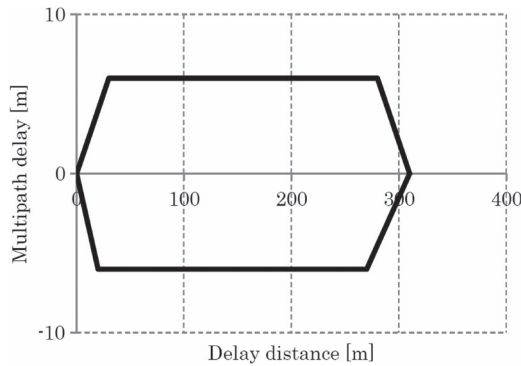
Fig. 2. The theoretical multipath envelope of narrow correlator [15].

According to [24], the pseudorange caused by NLOS is normally within a few hundred meters and potentially unbounded. Thus, this paper focuses on the mitigation of NLOS reception.

C. An Example of GPS Receiver in Urban Canyon

As mentioned in the introduction, various methods have been developed to identify NLOS satellites. It is easy for those techniques to identify signal's visibility but not easy to estimate the pseudorange delay. Thus, the detected suspicious pseudoranges are generally excluded from the position calculation to avoid the adverse effects. However, such method requires a large number of satellites because the rejection of NLOS signals decreases the available satellites in the calculation. Urban areas contain many tall buildings. Signals from satellites are often reflected or completely blocked. As a result, the number of directly visible satellites often becomes less than four. A GPS receiver requires at least four satellites to calculate the position in three dimensions. Fig. 3 shows an example of the number of LOS GPS satellites observed at Hitotsubashi, Chiyoda-ku, Tokyo. The Ray-tracing method [16] is utilized to count the number of LOS satellite. This graph reveals that the lack of satellites in urban areas. Clearly, there is two-third of the time that less than four satellites in view. This shortage of satellites reduces the positioning accuracy and availability.

One global trend is to use multiple GNSSs to increase the performance. In the near future, satellite navigation systems are expected to become more commonly available with the launch of multiple GNSSs, such as Chinese BeiDou system, European GALILEO system, Indian Regional Navigational Satellite System, and Japanese Quasi-Zenith Satellite System. However, currently the number of portable device with GPS modules is more than that of portable device with multiple GNSS modules. The authors recognize the importance of optimizing the existing low-cost, stand-alone, single-frequency GPS devices. Therefore, this paper focuses on the study of taking advantage of NLOS signal, which regards the NLOS signal as an additional measurement of the GPS receiver, instead of excluding it. The detail will be introduced in Section IV.

III. MULTIPATH AND NLOS DETECTION BY 3-D MAP

A. 3-D Building Map

In order to apply the ray-tracing simulation, the construction of a 3-D building map is needed. To establish the 3-D
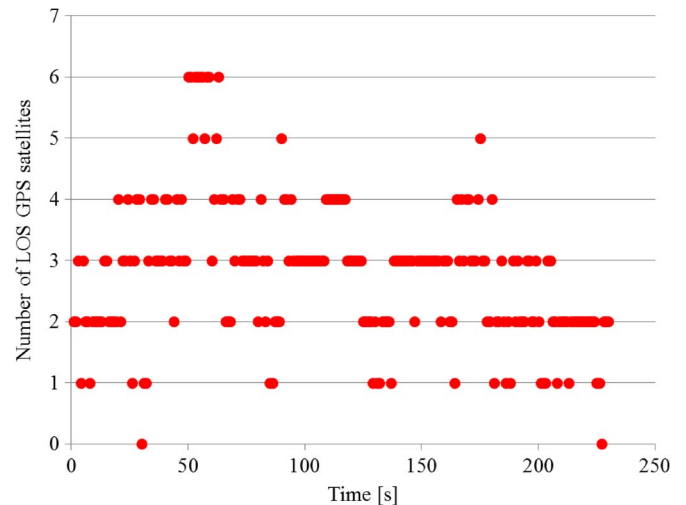

Fig. 3. Example of number of LOS GPS satellites observed in Tokyo, Japan.

building map, a 2-D map that contained building location and the height information of buildings are required. The Fundamental Geospatial Data (FGD) of Japan, which was provided by Japanese geospatial information authority and is open to Japanese public. This FGD data is employed as 2-D geographic information system (GIS) data. Thus, the layouts and positions of every building on the map could be obtained from the 2-D GIS data. In this paper, the 3-D digital surface model (DSM) data is provided by Aero Asahi Corporation. Fig. 4 shows the process of constructing the 3-D building map used in this paper. This paper first extracts the coordinates of every corner of buildings from FGD as shown in Fig. 4(a). Afterwards, the 2-D map is integrated with the height data from DSM with it. Fig. 4(b) illustrates an example of a 3-D building map that established in this paper. This simple 3-D building map is utilized in the simulation of ray-tracing.

This paper selects the Hitotsubashi area in Tokyo to constructs the 3-D building map because of the density of the tall buildings. Multipath and NLOS effect are frequently observed. Thus, the GPS positioning accuracy is very poor in this area. In this paper, tests were performed at the pedestrian walks and a road intersection. The landscape of the road and the ray-tracing simulation are shown in Fig. 5. Due to the buildings at the both sides of the road, the received signals indicated by the green lines are reflected. This reflection could be regarded as NLOS signal. In addition, the developed 3-D building map contains very small amount of data for each building in comparison to that of the 3-D graphic application. This paper only contains the frame data of each building instead of the detail polygons data of building. An accurate 3-D building map is measured by the Mobile Mapping System (MMS) as a reference. The average 2-D position difference between the reference and our developed 3-D models is about 0.5 meter. This result indicates the accuracy of the developed 3-D building model is capable of estimating the reflection path of GPS signal.

B. Ray Tracing

Ray tracing is a technique originally used in the field of computer graphics to generate an image of an object by tracing

(a)
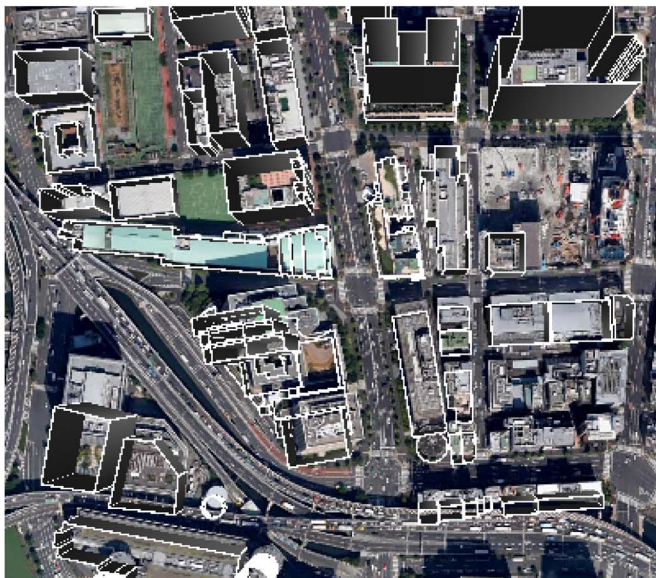
(b)

Fig. 4. The construction of the 3D building map from a 2D map and DSM. (a) 2D map. (b) 3D building map.

Fig. 5. Ray-tracing simulation for multipath estimation.
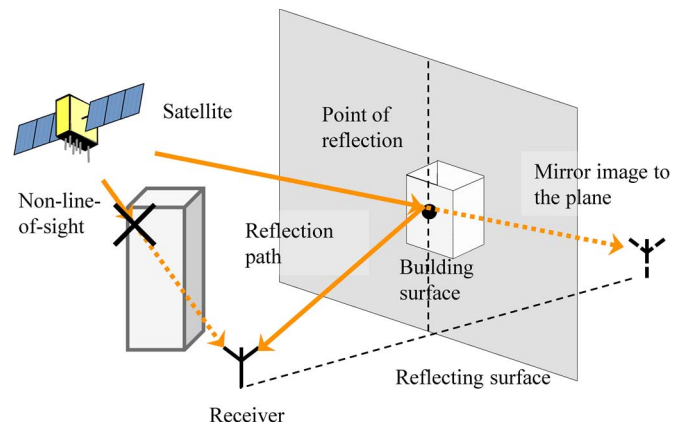
Fig. 6. The ray tracing technique used in this paper.

the path of light. Currently, ray tracing is also used to simulate radio propagation [25], [26]. This paper does not consider diffractions or multiple reflections because these signals occur under unfavorable conditions. Thus, this paper only utilizes the direct path and a single reflected path. If there are more than one reflection, this paper considers only the shortest reflection because its effects are usually higher than others.

An example of the combination of the GPS signal propagation simulation using ray tracing and a 3-D building map is shown in Fig. 5. Red, green and white lines denote the LOS path, reflected paths and the NLOS paths, respectively. White lines are signals in which ray tracing could not find any paths between the ground reference position and the satellite position. The developed ray-tracing simulation can be used to distinguish reflected rays and to estimate the reflection delay
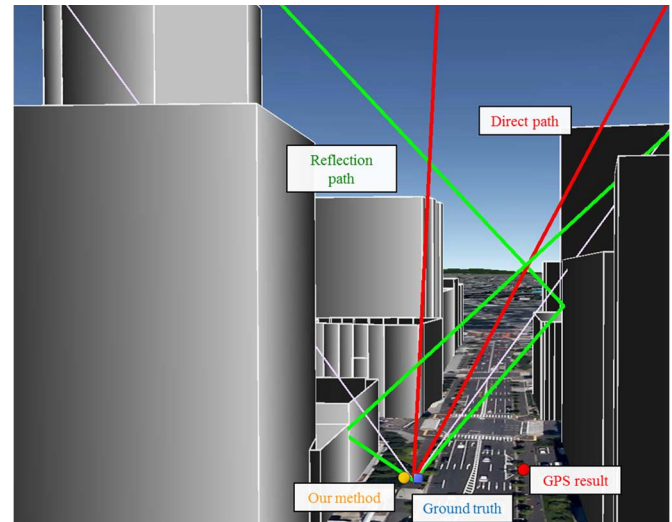
distance. This paper assumes that the surfaces of buildings are reflective smooth planes, namely mirrors. Therefore, the rays in the simulation obey the laws of reflection. In real world, the roughness and the absorption of the reflective surface might cause the mismatch between the ray-tracing simulation and the real propagation. This paper neglects this effect due to the roughness of the building surface is much smaller compared to the propagation distance. The algorithm employed to find a reflection path is described in Algorithm 1 and illustrated in Fig. 6.

C. Uncertainty in the Building Edge

Because there is an uncertainty in both the 3-D DSM data and 2-D GIS data, there is also an uncertainty in the constructed 3-D building map. This uncertainty might lead to incorrect LOS/NLOS estimation. Thus, the possibility of false detection of multipath must be considered, especially when a signal ray passes through nearby buildings or when a ray is blocked by the edges of a buildings as shown in Fig. 7.

Algorithm 1 Finding a reflection path

STEP1: Compute the receiver's mirror image position to a building surface.

STEP2: Prepare a line segment connecting the mirror image and a satellite.

STEP3: Calculate an intersection of the line segment and a plane consisting of the building surface.

STEP4: If the intersection is outside of the surface, reflected path does not exist from the building.

STEP5: If not, prepare two line segments connecting the point of reflection and the satellite, and the point of reflection and the receiver.

STEP6: If both of line segments are not blocked by some other structures, they are considered as a reflected path.

In order to mitigate the incorrect NLOS determination, this paper defines the minimum distance between the wall of a building and a direct signal path as a parameter. The distance is called the minimum distance in this paper. The minimum distance is calculated by the ray-tracing simulation. If the minimum distance $d_{\min}$ is larger than a threshold distance ($d_{\min}^{thres}$), the direct signal path is identified as a LOS signal. Conversely, if $d_{\min}$ is smaller than $d_{\min}^{thres}$, the LOS/NLOS determination is examined by the received signal strength. In this examination of received signal strength, the signal is considered as a LOS if it is sufficiently strong compared to the average signal strength. On the contrary, the sufficiently weak signals are considered NLOS. The threshold distance is determined on the basis of the accuracy of the 3-D building maps. The resolution of the 2-D GIS data obtained from Japan geospatial information authority and 3-D DSM data from Aero Asahi Corporation are 2 m and 1 m, respectively. Thus, $d_{\min}^{thres}$ is defined as 3 m in this study.

IV. PROPOSED ALGORITHM

This paper proposes an algorithm to estimate the receiver position by the use of the measured raw pseudoranges, the 3-D building map and ray tracing technique. The proposed method first distributes a number of positioning candidates, evaluates the candidates' feasibility and then calculates proper likelihood function of the feasible candidates. Finally, the expected value of all the candidates is regarded as the rectified receiver position. The following details each step of the proposed method.

A. Position Candidates

The output rate of the proposed method is based on the output rate of the commercial GPS receiver. The receiver outputs the measured raw pseudorange set $\rho = [\rho_1, \rho_2, \ldots, \rho_n]^T$ and the reference position y_{GPS} calculated by the commercial GPS receiver. It is important to note that the proposed method can give a position estimate only if there are more than four raw pseudoranges from GPS satellites. The proposed method distributes many position candidates $P^{(i)}$, where i denotes the index of candidates. The candidates are distributed as a grid around the initial position, which is the positioning result
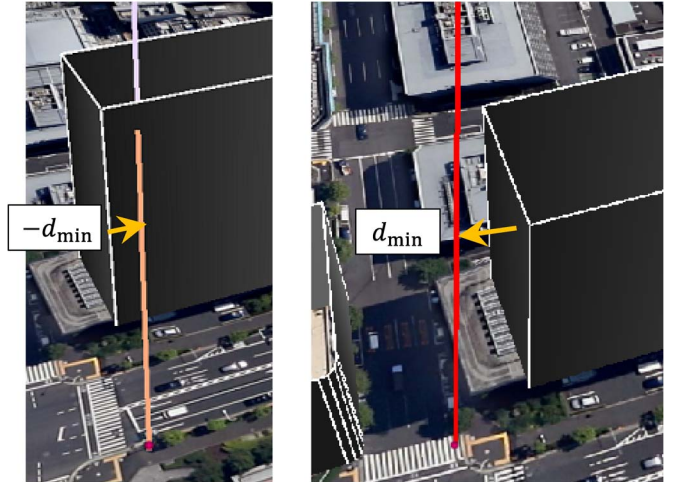

Fig. 7. An example of the minimum distance defined in this paper.

from GPS receiver. This paper assumes that the ground-truth is located within 30 m of the GPS result $y_{\mathrm{GPS}}(t)$ most of the time. Based on this assumption, the grid size is set to 50 m, and the grid width is 1 m. An example of the grid and candidates is shown in Fig. 8. Note that if the ground-truth is not within 30 m of the initial position, the proposed method cannot give accurate positioning result in this case.

B. Simulated Pseudorange From a Candidate

Assuming $P^{(i)}$ as the ground reference position, the possible reflection delay distance (namely the NLOS delay) $\varepsilon_n^{\mathrm{refl}}$ from $P^{(i)}$ to each satellite can be estimated by ray tracing. Thus, a simulated pseudorange between candidate $P^{(i)}$ to the nth satellite x_n^{sv}, $\widehat{\rho}^{(i)} = [\widehat{\rho}_1^{(i)} \widehat{\rho}_2^{(i)} \ldots \widehat{\rho}_N^{(i)}]^T$, can be calculated by summing the geometric distance $R_n^{(i)} = \|x_n^{\mathrm{sv}} - P^{(i)}\|$, the satellite clock offset equivalent distance $c\delta t_n^{\mathrm{sv}}$, the receiver clock offset equivalent distance $c\delta t^{\mathrm{r}(i)}$, the ionospheric delay I_n, the tropospheric delay T_n, and the reflection delay distance $\varepsilon_n^{\mathrm{refl}(i)}$. The bold symbol denotes the vector form of variable in this paper.

$$\widehat{\rho}^{(i)} = \left[\widehat{\rho}_1^{(i)} \widehat{\rho}_2^{(i)} \ldots \widehat{\rho}_N^{(i)} \right]^T$$
$$= R^{(i)} + c \left(\delta t^{\mathrm{r}}(i) - \delta t^{\mathrm{sv}} \right) + I + T + \varepsilon^{\mathrm{refl}(i)}. \quad (2)$$

In the proposed method, the satellite clock offset δt^{sv} is corrected using the broadcast ephemeris. The ionospheric delay I is obtained from the Klobuchar model. The tropospheric delay T is calculated based on the Saastamoinen model. The receiver clock offset $\delta t^{\mathrm{r}(i)}$ is modified to minimize the difference between the simulated set and the observed set.

If the simulated pseudorange set is affected by signal reflections in the same way as the observed pseudorange set is, the simulated pseudorange set should be similar to the observed set. By using these two sets of pseudoranges, the similarities between the observed pseudorange set ρ and the simulated pseudorange set $\widehat{\rho}^{(i)}$ can be evaluated. If the two pseudorange sets are very similar, the position of the candidate
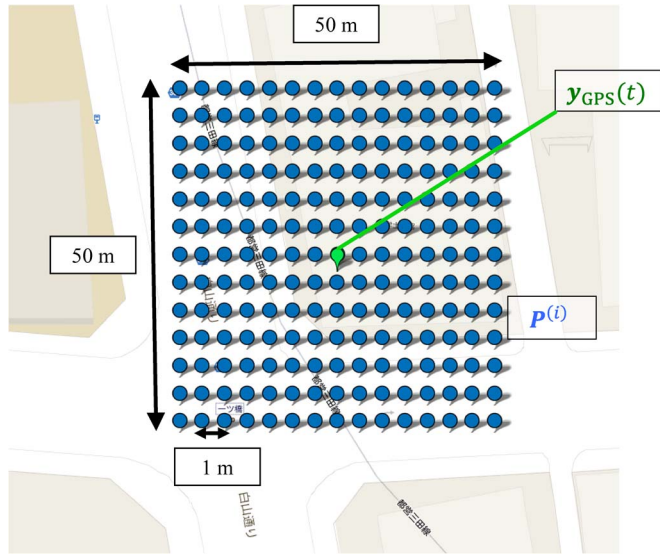
Fig. 8. Example of position candidates (blue circles) around the GPS result.

is highly likely to be close to the ground-truth. The pseudorange difference $(D_{pr}^{(i)})$ is defined as follows:

$$D_{pr}^{(i)} = \frac{1}{N^{\mathrm{sim}}} \times \min_{\delta t^{\mathrm{r}(i)}} \sum_n^{N^{\mathrm{sim}}} \left| \rho_n - \widehat{\rho}_n^{(i)} \left(\delta t^{\mathrm{r}(i)} \right) \right| \qquad (3)$$

where N^{sim} denotes the number of simulated pseudoranges. One should note that this pseudorange difference indicates the similarity between the observed and simulated pseudoranges. However, there is a situation that small values of the calculated pseudorange difference cannot represent high weightings of candidates. This paper only focuses on the mitigation of NLOS reception and does not mitigate multipath effects. If the observed pseudorange is highly affected by the multipath instead of NLOS, then the difference between the observed and simulated pseudorange will not be small.

C. Positioning Results Using the Simulated Pseudorange

In order to solve the multipath problem that mentioned earlier in the previous subsection, this paper also considers using the difference between the observed and simulated positions as a factor to calculate the likelihood function of candidates. In the case of that the multipath effect is larger than that of the NLOS, the observed position (namely the position result obtained from the commercial GPS receiver) is relatively reliable in comparison to the opposite situation. The reason for this behavior is that the commercial GPS receiver employs special correlators to mitigate the multipath. Thus, if the simulated position of a candidate is close to the observed position, then the candidate is given to a high confidence.

When the receiver outputs the measured raw pseudorange set, a position y_{GPS} can be calculated by WLS. A simulated position $\widehat{y}^{(i)}$ can be calculated by the WLS calculation using the simulated pseudorange set of a candidate. The illustrations of observed position, y_{GPS}, and simulated position, $\widehat{y}^{(i)}$ are shown in Fig. 9. Fig. 9(a) illustrates an example of the ob-
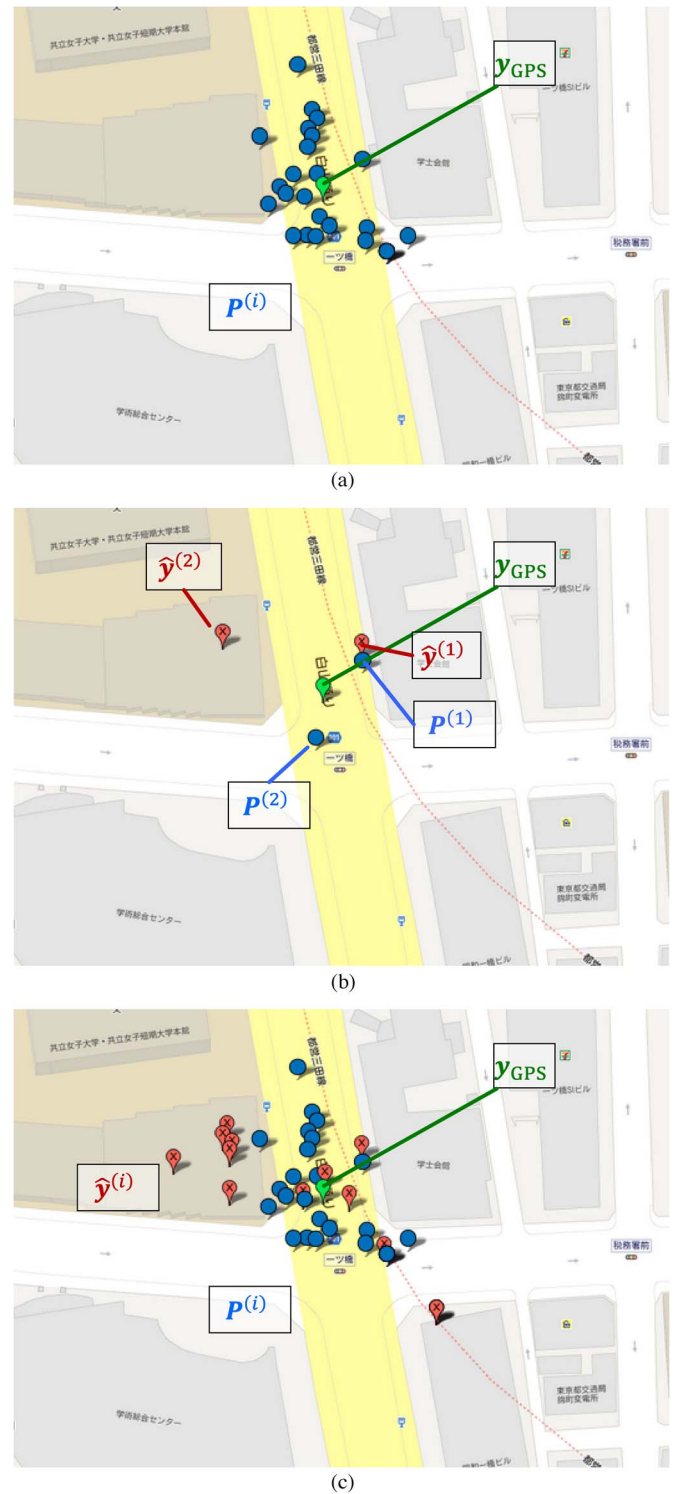

Fig. 9. Examples of sampling and the evaluation process. The y_{GPS} refers to reference (observed) position from the receiver. (a) Examples of the reference position y_{GPS} and the sampling points $P^{(i)}$. (b) Examples of the calculated positions $\widehat{y}^{(1)}$ and $\widehat{y}^{(2)}$, the candidate points $P^{(1)}$ and $P^{(2)}$, and the reference position y_0. (c) Examples of every calculated position $\widehat{y}^{(i)}$ for $P^{(i)}$ overlaid on (a).

served position, y_{GPS}, and the candidates, $P^{(i)}$. Fig. 9(b) shows two example of candidates illustrated in Fig. 9(a) and the corresponding simulated positions, $\widehat{y}^{(i)}$. As shown in Fig. 9(b), the $\widehat{y}^{(1)}$ appears near the $P^{(1)}$, while $\widehat{y}^{(2)}$ appears far away from

$P^{(2)}$. The simulated positions $\widehat{y}^{(i)}$ for every candidates, $P^{(i)}$, in Fig. 9(a) are illustrated in Fig. 9(c). Based on the reasons above, this paper uses that the distance between y_{GPS} and $\widehat{y}^{(i)}$ to indicate the confidence of the candidates. The difference in the positioning results $(D_{pos}^{(i)})$ is defined as follows:

$$D_{pos}^{(i)} = \left\| y_{\text{GPS}} - \widehat{y}^{(i)} \right\|. \tag{4}$$

D. Evaluation of the Position Candidates

To use the calculated similarities, the conditions of the position candidates $P^{(i)}$ should be evaluated. First, the reasonability of NLOS detection according to signal strength is evaluated. $P^{(i)}$ can be one of the reasonable positions if it satisfies the following requirements.

$P^{(i)}$ should:

- be outside of any building if any carrier-to-noise ratio (C/N_0) is sufficiently strong,
- be directly visible (LOS) from satellites whose C/N_0 is sufficiently strong compared to the average C/N_0,
- and be NLOS, whose C/N_0 is sufficiently weak compared to the average C/N_0.

In this paper, the received signal strength and the average strength from the GPS receiver are utilized. Ten epochs are used to calculate the average C/N_0. It is important to note the C/N_0 is affected by the elevation angle. However, the proposed method of this paper is to develop a rectified positioning method in urban canyon environments. In this case, general speaking, the satellite with low-elevation angle is very difficult to be received. Even if the signals from low-elevation satellite are received, they usually received as reflected signal instead of LOS. Based on the reasons above, the authors believe that it is reasonable to use C/N_0 to distinguish the NLOS and LOS.

The candidates that satisfied the above requirements are selected to calculate the final position of the proposed method. It is important to note the weighting of each candidate should be different. The likelihood of the candidates is calculated on the basis of the two similarities discussed earlier in this section. The likelihood $\alpha^{(i)}(t)(i = 1, \cdots, N_p)$ for each candidate is determined by considering both the pseudorange and position similarities. The likelihood function is shown in the following:

$$\alpha^{(i)}(t) = L_{\text{pr}}^{(i)} \, L_{\text{pos}}^{(i)} \tag{5}$$

$$L_{\text{pr}}^{(i)} = \begin{cases} \exp\left[-\dfrac{D_{Pr}^{(i)2}}{\sigma_0^2}\right] & \left(\text{if } D_{pr}^{(i)} < C_1\right) \\ 0 & (\text{otherwise}) \end{cases} \tag{6}$$

$$L_{\text{pos}}^{(i)} = \begin{cases} \exp\left[-\dfrac{D_{pos}^{(i)2}}{\sigma_{\Delta t}^2}\right] & \left(\text{if } D_{pos}^{(i)} < C_2\right) \\ 0 & (\text{otherwise}) \end{cases}. \tag{7}$$

This paper assumes both the distributions of the similarities are Gaussian distributions. The first and second parts of the likelihood function, L_{pr} and L_{pos}, are based on the similarity of the pseudorange sets and the positioning results, respectively. In order to exclude the ridiculous candidate, this study defines

two constant threshold, C_1 and C_2, with values 8 m and 40 m, respectively. σ_0 and $\sigma_{\Delta t}$ are constant that stabilized the estimate and are determined empirically. Finally, the recertified positioning result of the proposed method is calculated by

$$x(t) = \frac{\sum_i \alpha^{(i)}(t) P^{(i)}(t)}{\sum_i \alpha^{(i)}(t)}. \tag{8}$$

In summary, the likelihood function evaluates the confidence of the candidates referring to both the reasonability of the simulated pseudorange the positioning result by the simulated pseudorange. The estimated position is calculated as a weighted average of the position candidates.

Algorithm 2 Position Estimation Algorithm

STEP1:   Every time the receiver outputs the raw pseudorange set ρ, calculated the reference position y_{GPS}.

STEP2:   Divide a 50 m $\times$ 50 m area around y_{GPS} into 50 $\times$ 50 grids represented by $P^{(i)}$. **do**

STEP3:   **for all** the candidates $P^{(i)}$ **do**

STEP4:   Estimate the LOS/NLOS condition and compute the reflection delay $\varepsilon^{\text{refl}}(i)$.

STEP5:   Calculate the simulated pseudorange set $\widehat{\rho}^{(i)}$ according to (2).

STEP6:   **if** the ray-tracing result does not contradict the received signal strength **then**

STEP7:   Compute the pseudorange difference $\text{diff}^{\text{pr}(i)}$ according to (3).

STEP8:   Compute the difference in positioning results $D_{pos}^{(i)}$ according to (4).

STEP9:   Compute the likelihood $\alpha^{(i)}$ according to (5)–(7).

STEP10: **end if**

STEP11: **end for**

STEP12: Set output $x(t) \leftarrow (\sum_i \alpha^{(i)}(t) P^{(i)}(t)) / (\sum_i \alpha^{(i)}(t))$

E. Smoothing by Particle Filter

In order to smoothen the trajectories of the estimated positions, a particle filter is employed for this purpose [13]. To use the particle filter, the design of the state dynamics model, state vector, and likelihood function are required to weight each particle. The observation is $x(t) = [\varphi(t), \lambda(t)]^T$, a 2-D coordinate position estimated above. The state vector is defined as $\widehat{x} = [\varphi, \lambda, v_\varphi, v_\lambda]^T$, where φ and λ respectively denote the latitude and longitude with corresponding velocities v_φ and v_λ. This paper assumes that the state propagation noise is Gaussian white noise, $N_t \sim \mathcal{N}(0, \Sigma)$. The state propagation model is expressed as follows:

$$\widehat{x}(t) = F\widehat{x}(t - \Delta t) + N_t \tag{9}$$

$$F = \begin{vmatrix} 1 & 0 & \Delta t & 0 \\ 0 & 1 & 0 & \Delta t \\ 0 & 0 & 1 & 0 \\ 0 & 0 & 0 & 1 \end{vmatrix}. \tag{10}$$

This filter is used by a set of particle samples $\boldsymbol{S}(t) = [\boldsymbol{s}^{(1)}(t), \boldsymbol{s}^{(2)}(t), \cdots, \boldsymbol{s}^{(N_p)}(t),]^T$. In filter updating process, the confidence $\pi^{(i)}(t)$ of sample is determined based on 2-D difference, a simple likelihood function:

$$\pi^{(i)}(t) = \frac{\left\| \boldsymbol{s}^{(i)}(t) - \boldsymbol{x}(t) \right\|}{\sum_{i}^{N_p} \left\| \boldsymbol{s}^{(i)}(t) - \boldsymbol{x}(t) \right\|}. \tag{11}$$

F. Improvement in Search Efficiency

The aim of this study is to provide a real-time accurate positioning algorithm. Hence, the computational load of the proposed method is also discussed. For the real-time application, the calculation time for each position estimate should be estimated. As discussed in Section IV, 2500 candidates need to be evaluated. The evaluation time of each candidate has to be shorter than 0.4 millisecond in order to achieve a position estimate within 1 second. However, it is less possible to evaluate each candidate with such a short time because the algorithm needs to calculate all possible traveling paths of the ray, which is highly complicated. Therefore, this paper further develops a random sampling method to reduce the required numbers of candidates. The random sampling method is based on the continuity of movement and the possibility of a dense location.

To reduce the number of candidate, the particles $\boldsymbol{p}^{(i)}$ are distributed around the reference positions instead of using grid points. Namely, the particles $\boldsymbol{p}^{(i)}$ are sampled around $\boldsymbol{y}_{\text{GPS}}(t)$. Each particle is considered as a position candidate. The distribution of the particles is determined on the basis of a 2-D Gaussian distribution to randomly place around the reference position. The behavior of the distribution is similar to typical GPS positioning errors. On the other hand, particles should also be placed around the previous estimated position $\boldsymbol{x}(t - \Delta t)$ because of the continuity of movement. Therefore, the resampling of particles are arranged to be suited to the situation. In this paper, the number of particles is 300. It is understandable that the proposed method can estimate more accurately with more particles. However, the more particles also consumes more computation loads. It is important to reach a balance between the accuracy and computation load. Based on the objective of real-time calculation, this paper selects 300 particles (with 8 satellites in view) in the proposed method to calculate the positioning result within 1 second. During the resampling phase, half of particles are generated according to a normal distribution $\mathcal{N}(\boldsymbol{y}_{\text{GPS}}(t), \sum_0)$, while the others are generated according to normal distribution $\mathcal{N}(\boldsymbol{x}(t - \Delta t), \sum_{\Delta t})$ based on the continuity of movement. The distribution of the resampling sample is shown in Fig. 10. The spread width for the first half of particles is arranged to 50 m due to the variance of the receiver positioning result. The spread width of the second half is set up based on both the uncertainty of previous position estimate and regular motion of pedestrian. In general, the 1-sigma positioning error of the proposed method is less than 10 m. The general pedestrian walking speed is regarded as 1 m/s. Thus, the spread width for the continuity of movement is 10 m in this paper.
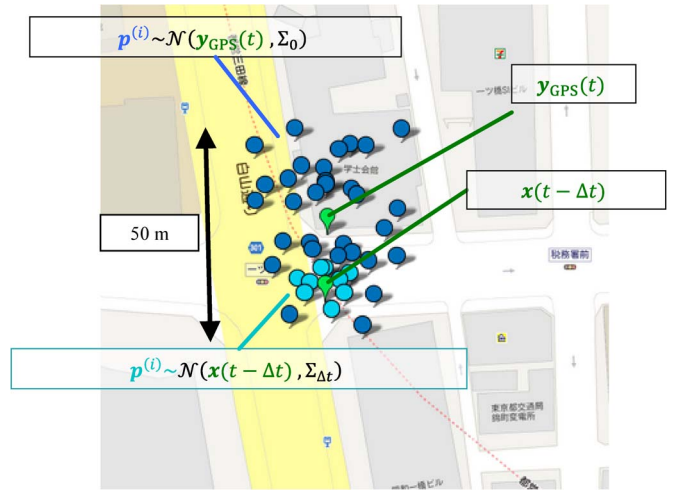

Fig. 10. Example of position candidates around the GPS result and around the previous estimate.

V. EXPERIMENTAL RESULTS

A. Equipment Setup

For the experiment, the necessary data from the GPS receiver are the raw ephemeris, the raw pseudorange set, the signal strength of each satellite and the calculated position outputs.

This work employs a u-blox NEO-6P GPS Evaluation Kit, which is a simple, small, low-cost, standalone and single frequency GPS L1 receiver. The antenna used in the experiment is the u-blox ANN-MS active antenna, namely a patch antenna, with 5-m cable. The u-blox receiver output rate is 1 Hz. This paper also collects the positioning result from an iPhone 4S mobile to understand the performance of current mass-market merchandise.

In the first test, the quasi-ground-truth trajectory was obtained on the basis of where the pedestrian actually walked. In the second test, this paper employs video cameras to capture the trajectories of the pedestrian with the receiver. Video cameras were installed on the upper floor of a building near the experimental site. The quasi-ground-truth positions were estimated by comparing the captured video and high-resolution orthophotography. The orthophotography resolution was 25 cm/pixel. Therefore, the error distance for each estimate can be calculated.

B. Efficiency Evaluation of the Particle Sampling

This paper evaluates the calculation time of the proposed algorithm using a grid sampling method and a particle sampling method. For a quantitative evaluation, the average calculation time and the error distance of the position estimation algorithms are measured. During the tests, a laptop computer with Intel Core i7 2.70 GHz is employed. The source code is written in C++. The error distance is defined as the distance from the quasi-ground-truth line to each estimated position. Because these error distances are calculated from a line, not from each quasi-ground-truth point, the values do not exactly represent the error of each estimated point. However, we believes that this error value can still evaluate the minimum required

TABLE I
MEAN CALCULATION TIME AND ERROR DISTANCE
OF THE POSITION ESTIMATION

Case	Mean Calculation Time [ms]	Mean Error [m]
Grid search	2034	5.8
Particle search	310	5.6

performance. The results are summarized in Table I. To further evaluate the computational load that reduced by the particle sampling method, this paper compares the computational load of the two methods. The heaviest computational load of the proposed method is the ray-tracing.

First, all the buildings are assumed to be shaped as simple rectangle. M buildings would have $M \times 4$ planes. If there is N satellites are received by the receiver, then the number of ray-tracing calculation for a single candidate would be $M \times 4 \times N$. In the paper, the number of candidate reduced by particle sampling method is 2200 candidates. Thus, the total reduced ray-tracing calculation is $M \times 4 \times N \times 2200$, which significantly reduces the processing load.

Comparing the positioning error of the two sampling method the positioning performance is almost the same, while the calculation time of the particle search is much shorter than the grid search. Therefore, for following experiments, this paper uses the proposed algorithm with the particle sampling method. Step 2 of Algorithm 2 is modified to the following step:

STEP2: Generate half of the position assumptions (particles) around $\boldsymbol{y}_{\text{GPS}}$ according to the normal distribution $\mathcal{N}(\boldsymbol{y}_{\text{GPS}}(t), \sum_0)$ with a 50-m spread width. If the previous estimate exists, generate the other half of the assumptions around $\mathbf{x}(t - \Delta t)$ according to the normal distribution $\mathcal{N}(\boldsymbol{x}(t - \Delta t), \sum_{\Delta t})$ with a 10-m spread width.

C. Walking Straight Along a Sidewalk: Test 1

First field test was conducted in January 2013 at the Hitotsubashi intersection mentioned in Section III-A. This test was operated for a rough evaluation of the proposed method. Fig. 11 shows an example of the trajectories of the first test. The green line, red circles, and yellow squares on the map represent the results from an iPhone4S, a u-blox NEO-6P, and the proposed method, respectively. In this case, a p pedestrian carrying the receivers moved along the sidewalk from the lower right to the top middle of the picture. This route is approximately 250 m and takes about 180 s to travel. In contrast to the iPhone and u-blox receiver, the result of the proposed method is closer to the quasi-ground-truth trajectory. In addition, the result of the proposed method does not appear on the wrong side of the road, while other two devices often appear on the opposite side of the road. Each quasi-ground-truth position is not recorded with time clock information, thus the evaluation of the error distance for this test is qualitative.
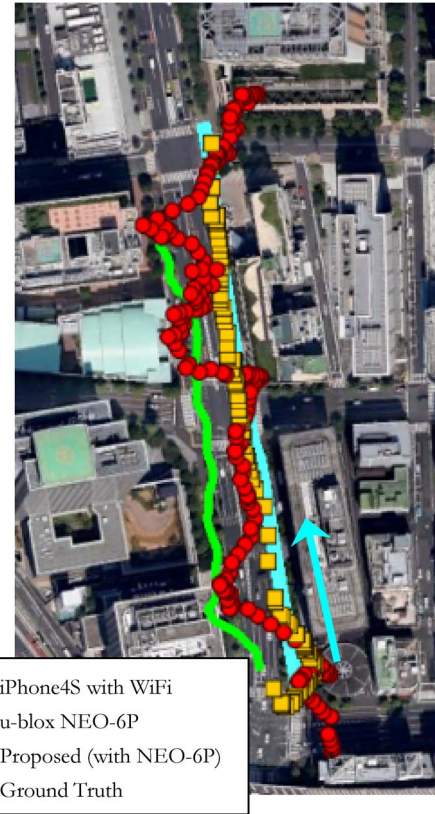

Fig. 11. Examples of the positioning results, the trajectories of the commercial GPS receiver (red circles, green line), and the proposed method (yellow squares). The cyan line indicates the true route.

### D. Walking Around an Intersection: Test 2

The second field tests were conducted in August 2013 at the same place mentioned in Section III-A.

The experimental results of the proposed method with/without filter and commercial GPS receivers are shown in Fig. 12. As mentioned earlier, this paper employs a particle filter to smooth the output and to exclude points that located far away from the previous estimate.

E. Evaluation

As observed in Fig. 12, the estimated trajectory by the proposed method is much more similar to the quasi-ground-truth than that of the commercial GPS receivers. Both iPhone 4S and u-blox NEO-6P receivers give distorted trajectories.

It is interesting to note the trajectories given by the two commercial receivers are similar. The reason for this phenomenon is the reception of NLOS signals. As mentioned earlier, the commercial receiver is not capable of mitigating the effect of NLOS signal. Fig. 5 demonstrates a snapshot of the ray-tracing simulation of the experiment result. The quasi-ground-truth, the GPS result and the proposed method are denoted by the cyan, red and yellow dots, respectively. As shown in the Fig. 5, the GPS result is far away from the quasi-ground-truth because of the two signal reflections, which indicated by the green lines. In contrast, the proposed method successfully estimates the two reflection paths and two direct paths, so that the estimate is very close to the quasi-ground-truth. To compare the left and right of
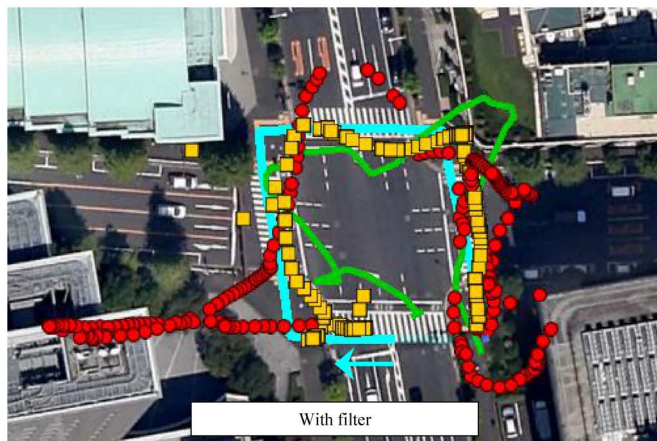
(a)
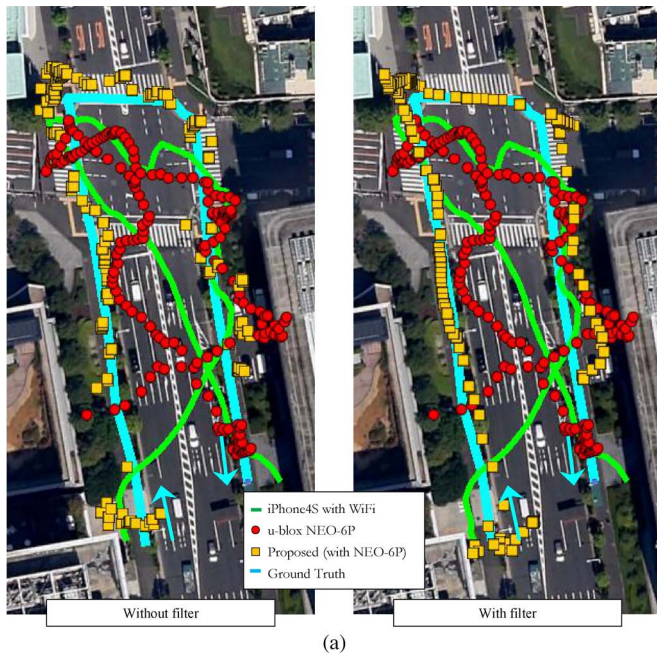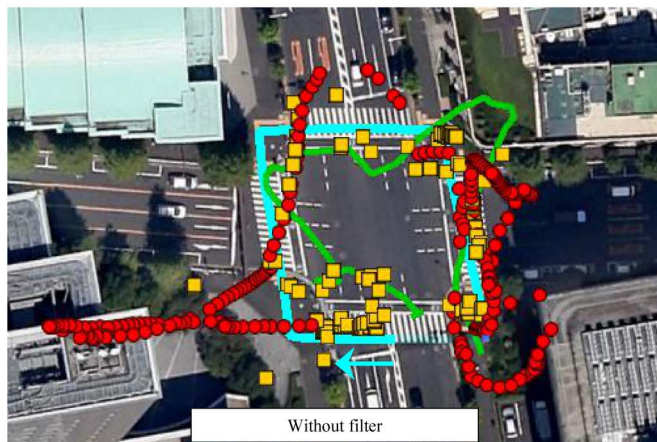
(b)

Fig. 12. Comparison of the positioning trajectories between the commercial GPS receiver (red circles, green line) and the proposed method (yellow squares). A particle filter is utilized for smoothing. The cyan line indicates the true ground route. (a) Test 2-Case1. (b) Test 2-Case2.

Fig. 12(a), the performance of the proposed method is highly improved by the particle filter. Again, the improvement can be observed from Fig. 12(b). However, it is not clear and fair to
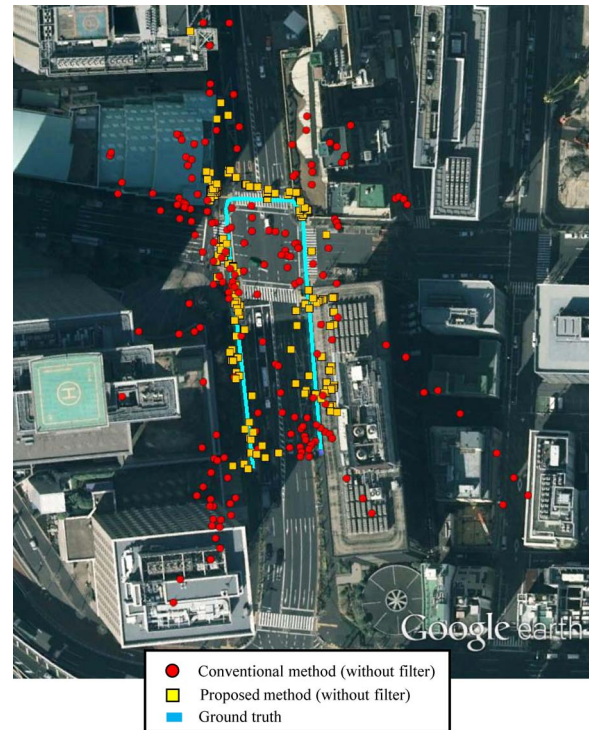

Fig. 13. Comparison of the positioning trajectories between the conventional methods (red circles, green line) and the proposed method (yellow squares).

compare the filtered positioning results from the commercial GPS receiver and the proposed method due to different types of filter are used. This difference can be seen by comparing the availability. The proposed method only calculates the positioning if the numbers of available satellite are more than four. However, the GPS positioning result from the u-blox receiver somehow used filters to smooth the positioning results. Even if there are no signals from satellites for a second, the u-blox receiver can still output a positioning result. Based on the reasons above, the yellow dots are less than red dots in Figs. 10–12. During the tests, the percentage of the time that more than four GPS satellites are in LOS area is approximately 25%. In contrast to this, the availability of the proposed method is approximately 71%; and GPS itself is approximately 91%. Although the proposed method also used a particle filter to smooth the result, this particle filter only helps the proposed in the distribution of the particles (candidates) instead of smoothing the position results when the signal outage. If the number of valid satellite is less than four, the proposed will not give a position. In order to fairly compare the u-blox receiver and the proposed method, this paper calculates the results using the raw pseudorange and ephemeris by means of weighted least square method (namely a conventional method). The results are shown in Fig. 13 and 14.

In Fig. 13, it is difficult to identify the trajectory from the positioning results of the conventional method. In contrast, the proposed method could roughly obtain the trajectory. For a quantitative error evaluation, this paper considers the error distance as the distance from the quasi-ground-truth position to each estimated position. Fig. 14 draws the errors through the unfiltered and filtered tests. In Table II, the maximum, the
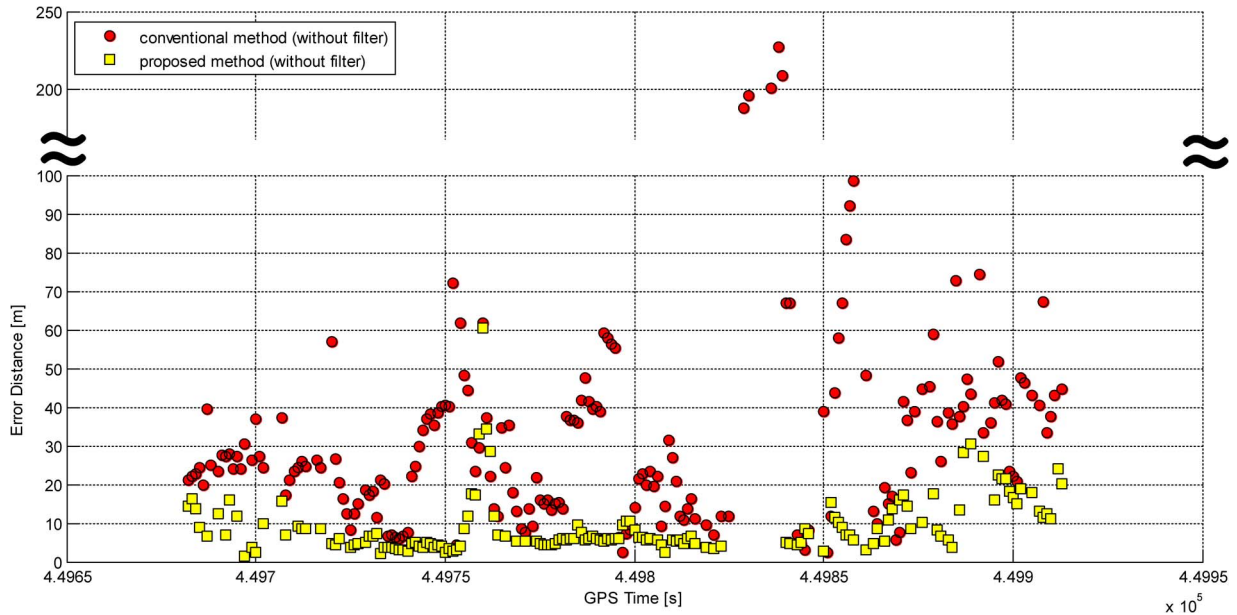
Fig. 14. Comparison of error distance between the conventional method (red dots) and the proposed method (yellow squares).

TABLE II
MAXIMUM, MEAN, AND STANDARD DEVIATION OF THE ERROR
DISTANCE OF THE AVERAGE AMONG THE TESTS

Case		Maximum Error [m]	Mean Error [m]	Standard Deviation [m]
Without smoothing	Conventional	227.2	34.6	34.3
	Proposed	60.4	9.2	7.7
With smoothing	Conventional	54.5	19.8	14.2
	Proposed	33.1	5.2	4.4

mean and the sample variance of error distances of the average among tests are shown. This result shows that by using the proposed method, the maximum of the error can be reduced from 54.5 to 33.1 m; the mean error from 19.8 to 5.2 m. It is interesting to note there are more epochs available for the conventional method. The proposed method estimates the positioning results based on the expectation calculation of all the position candidates (particles) as shown in equations (6)–(9).

As shown in the equation (7) and (8), if we fail to find any particle, which can fit both $D_{pr}^{(i)} < C_1$ and $D_{pos}^{(i)} < C_2$, then the proposed method cannot output a positioning result at that epoch. Thus, in general, the conventional method is capable of giving more results than the proposed method.

VI. CONCLUSION

This paper proposes an algorithm that uses 3-D building map and ray-tracing simulation to improve the accuracy of mobile GPS devices. Ray tracing only requires extra computational power with no additional device, so that the proposed method are even possibly applicable in portable devices. NLOS satellites can be identified by ray-tracing simulation and 3-D building map. The potential reflection delay distance from any

point in the area, where 3-D map is provided, can be also estimated. Thus, the simulated pseudorange of a candidate can be generated to evaluate the similarity between the simulated pseudorange set and the observed pseudorange set.

The difference between the two sets of pseudorange is regarded as a confidence of the position candidate. This difference is used in the calculation of the likelihood function. A particle filter with a proper state propagation model is also utilized to smooth the positioning result of the proposed method. In order to reduce the computational load of the proposed method, a random sampling method is utilized to distribute the effective samples. The position candidates are generated around the GPS result and the previous estimate. The calculation time is also evaluated and is found to be fast enough for the real-time estimations. The proposed method was evaluated through field experiments. According to the experiment results, the positioning accuracy improves dramatically in comparison to the conventional method.

In the experiment, the error distances are within 8 m at most of the points. However, some points still deviate from the actual ground position. These points in certain area are able to be estimated by the proposed method. The causes of these remaining errors and the causes of the failure of estimate will be investigated. Basically, the remaining error is mainly based on numerous errors which are not fully corrected by our model, such as ionospheric delay, tropospheric delay, and the error of 3-D building map. On the other hand, the cause of failure is mainly based on the failure of path-finding by ray-tracing simulation.

REFERENCES

[1] E. D. Kaplan and C. J. Hegarty, *Understanding GPS: Principles and Applications*. Norwood, MA, USA: Artech House, 2005.
[2] A. Yasuda, "Aspect of GPS Technology," (in Japanese), *IEICE Trans. B*, vol. J84-B, no. 12, pp. 2082–2091, Dec. 2001.
[3] G. MacGougan *et al.*, "Performance analysis of a stand-alone high-sensitivity receiver," *GPS Solutions*, vol. 6, no. 3, pp. 179–195, Dec. 2002.

[4] L. Garin and J. M. Rousseau, "Enhanced strobe correlator multipath rejection for code & carrier," in *Proc. 10th Int. Tech. Meet. Satellite Div. Inst. Navigat.*, Kansas City, MO, USA, 1997, pp. 559–568.

[5] A. J. Van Dierendonck, P. Fenton, and T. Ford, "Theory and performance of narrow correlator spacing in a GPS receiver," *J. Inst. Navigat.*, vol. 39, no. 3, pp. 265–284, 1992.

[6] B. Townsend and P. Fenton, "A practical approach to the reduction of pseudorange multipath errors in a L1 GPS receiver," in *Proc. 7th Int. Tech. Meet. Satell. Div. Inst. Navigat.*, Salt Lake City, UT, USA, 1994, pp. 143–148.

[7] M. S. Braasch, "Performance comparison of multipath mitigating receiver architectures," in *Proc. IEEE Aerosp. Conf.*, 2001, vol. 3, pp. 1309–1315.

[8] B. R. Townsend, P. C. Fenton, K. J. Van Dierendonck, and D. J. R. Van Nee, "Performance evaluation of the multipath estimating delay lock loop," *J. Inst. Navigat.*, vol. 42, no. 3, pp. 503–514, Fall 1995.

[9] P. C. Fenton and J. Jones, "The theory and performance of NovAtel Inc.'s vision correlator," in *Proc. 18th Int. Tech. Meet. Satell. Div. Inst. Navigat.*, Long Beach, CA, USA, 2005, pp. 2178–2186.

[10] R. G. Brown, "A baseline GPS RAIM scheme and a note on the equivalence of three RAIM methods," *J. Inst. Navigat.*, vol. 39, no. 3, pp. 301–316, 1992.

[11] Y. C. Lee and D. G. O'Laughlin, "A performance analysis of a tightly coupled GPS/inertial system for two integrity monitoring methods," *J. Inst. Navigat.*, vol. 47, no. 3, pp. 175–190, 2000.

[12] T. Iwase, N. Suzuki, and Y. Watanabe, "Estimation and exclusion of multipath range error for robust positioning," *GPS Solut.*, vol. 17, no. 1, pp. 53–62, Jan. 2013.

[13] F. Peyret, D. Bétaille, M. Ortiz, S. Miquel, and L. Fontenay, "How to improve GNSS positioning Quality of Service for demanding ITS in city environments by using 3D digital maps," in *Proc. 19th ITS World Congr.*, Vienna, Austria, 2012, pp. EU00077:1–EU00077:8.

[14] C. Pinana-Diaz, R. Toledo-Moreo, D. Betaille, and A. F. Gomez-Skarmeta, "GPS multipath detection and exclusion with elevation-enhanced maps," in *Proc. IEEE Intell. Transp. Syst. Conf.*, 2011, pp. 19–24.

[15] N. Kubo, A. Yasuda, and R. Shibazaki, "An effective multipath mitigation technique under strong multipath environments," in *Proc. Int. Symp. GNSS/GPS*, 2005, pp. 8–10.

[16] M. Obst, S. Bauer, P. Reisdorf, and G. Wanielik, "Multipath detection with 3D digital maps for robust multi-constellation GNSS/INS vehicle localization in urban areas," in *Proc. IEEE Intell. Veh. Symp.*, 2012, pp. 184–190.

[17] J. Meguro, T. Murata, J. Takiguchi, Y. Amano, and T. Hashizume, "GPS multipath mitigation for urban area using omnidirectional infrared camera," *IEEE Trans. Intell. Transp. Syst.*, vol. 10, no. 1, pp. 22–30, Mar. 2009.

[18] J. Marias, M. Berbineau, and M. Heddebaut, "Land mobile GNSS availability and multipath evaluation tool", *IEEE Trans. Veh. Technol.*, vol. 54, no. 5, pp. 1697–1704, Sep. 2005.

[19] Z. Jiang and P. D. Groves, "NLOS GPS signal detection using a dual-polarisation antenna," *GPS Solut.*, vol. 18, no. 1, pp. 15–26, Jan. 2014.

[20] P. D. Groves, "Shadow matching: A new GNSS positioning technique for urban canyons," *J. Navigat.*, vol. 64, no. 3, pp. 417–430, 2011.

[21] L. Wang, P. D. Groves, and M. K. Ziebart, "Urban positioning on a smartphone: Real-time shadow matching using GNSS and 3D city models," *Inside GNSS*, no. Nov/Dec, pp. 44–56, May/Jun. 2013.

[22] L. Wang, P. D. Groves, and M. K. Ziebart, "GNSS shadow matching: Improving urban positioning accuracy using a 3D city model with optimized visibility scoring scheme," *J. Inst. Navigat.*, vol. 60, no. 3, pp. 195–207, 2013.

[23] L. Wang, P. D. Groves, and M. K. Ziebart, "Smartphone shadow matching for better cross-street GNSS positioning in urban environments," *J. Navigat.*, vol. 68, no. 3, pp. 411–433, 2014.

[24] P. D. Groves, *Principles of GNSS, Inertial, and Multi-Sensor Integrated Navigation Systems (GNSS Technology and Applications)*. Norwood, MA, USA: Artech House, 2013.

[25] H. L. Bertoni, *Radio Propagation for Modern Wireless Systems*. New York, NY, USA: Pearson Education, 1999.

[26] M. F. Iskander and Z. Yun, "Propagation prediction models for wireless communication systems," *IEEE Trans. Microw. Theory Tech.*, vol. 50, no. 3, pp. 662–673, Mar. 2002.

Shunsuke Miura received the B.S. degree in applied physics from The University of Tokyo, Tokyo, Japan, in 2012. He is currently working toward the M.S. degree at The University of Tokyo.

His research interests include automotive driving technology, safety applications, and positioning for ITS.

Li-Ta Hsu received the B.S. and Ph.D. degrees in aeronautics and astronautics from National Cheng Kung University, Tainan, Taiwan, in 2007 and 2013, respectively.

He is currently a Japan Society for the Promotion of Sciences Postdoctoral Fellow with the Institute of Industrial Science, The University of Tokyo, Tokyo, Japan. In 2012, he was a Visiting Ph.D. Student with the Faculty of Engineering, University College London, London, U.K. He is the author or coauthor of more than 25 papers. His research interests include all aspects of GNSS navigation, positioning, and signal processing, including wide-area differential GNSS systems and improving GNSS performance under challenging reception conditions, and indoor positioning techniques.

Feiyu Chen received the B.S. degree in network engineering from the Beijing University of Post and Telecommunications, Beijing, China, in 2012. He is currently working toward the M.S. degree at The University of Tokyo, Tokyo, Japan.

His research interests include pedestrian positioning in urban areas with GPS and pedestrian dead reckoning.

Shunsuke Kamijo (M'97) received the B.S. and M.S. degrees in physics and the Ph.D. degree in information engineering from The University of Tokyo, Tokyo, Japan, in 1990, 1992, and 2001, respectively.

In 1992, he worked with Fujitsu Ltd., as a Processor Design Engineer. Since 2001, he has been with The University of Tokyo, where he served as an Assistant Professor until 2002 and is currently an Associate Professor. His research interests include computer vision for traffic surveillance by infrastructure cameras and onboard cameras, cooperative systems using V2X communication, GNSS and smartphone applications for ITS, and marketing.

Dr. Kamijo is a member of the International Program Committee of the ITS World Congress, The Institute of Electronics, Information and Communication Engineers, the Society of Automotive Engineers of Japan (JSAE), the Japan Society of Civil Engineers, and the International Association of Traffic and Safety Sciences. He is an Editorial Board Member of the *International Journal on ITS research* (Springer) and *Multimedia Tools and Applications* (Springer).